Biochimica et Biophysica Acta 1859 (2016) 719–730

Contents lists available at ScienceDirect

Biochimica et Biophysica Acta

journal homepage: www.elsevier.com/locate/bbagrm

DEAD-box RNA helicase DDX3 connects CRM1-dependent nuclear export and translation of the HIV-1 unspliced mRNA through its N-terminal domain

Alvaro Fröhlich [a,1], Bárbara Rojas-Araya [a,1], Camila Pereira-Montecinos [a], Alessandra Dellarossa [a], Daniela Toro-Ascuy [a], Yara Prades-Pérez [a], Francisco García-de-Gracia [a], Andrea Garcés-Alday [a], Paulina S. Rubilar [b,c,d], Fernando Valiente-Echeverría [a], Théophile Ohlmann [b,c,d], Ricardo Soto-Rifo [a,*]

[a] Molecular and Cellular Virology Laboratory, Virology Program, Institute of Biomedical Sciences, Faculty of Medicine, Universidad de Chile, Independencia 834100, Santiago, Chile
[b] CIRI, International Center for Infectiology Research, Université de Lyon, Lyon, France
[c] Inserm, U1111 Lyon, France
[d] Ecole Normale Supérieure de Lyon, Lyon, France

ARTICLE INFO

Article history:
Received 30 October 2015
Received in revised form 14 March 2016
Accepted 17 March 2016
Available online 21 March 2016

Keywords:
HIV-1
DDX3
Unspliced mRNA
CRM1
Nuclear export
Translation
Intrinsic disorder

ABSTRACT

DEAD-box RNA helicase DDX3 is a host factor essential for HIV-1 replication and thus, a potential target for novel therapies aimed to overcome viral resistance. Previous studies have shown that DDX3 promotes nuclear export and translation of the HIV-1 unspliced mRNA. Although the function of DDX3 during both processes requires its catalytic activity, it is unknown whether other domains surrounding the helicase core are involved. Here, we show the involvement of the N- and C-terminal domains of DDX3 in the regulation of HIV-1 unspliced mRNA translation. Our results suggest that the intrinsically disordered N-terminal domain of DDX3 regulates its functions in translation by acting prior to the recruitment of the 43S pre-initiation complex onto the viral 5′-UTR. Interestingly, this regulation was conserved in HIV-2 and was dependent on the CRM1-dependent nuclear export pathway suggesting a role of the RNA helicase in interconnecting nuclear export with ribosome recruitment of the viral unspliced mRNA. This specific function of DDX3 during HIV gene expression could be exploited as an alternative target for pharmaceutical intervention.

1. Introduction

DEAD (Asp-Glu-Ala-Asp)-box polypeptide 3, DDX3, is an ATP-dependent RNA helicase essential for Human Immunodeficiency virus type-1 (HIV-1) gene expression [1,2]. DDX3 was first reported as a host co-factor involved in the nuclear export of Rev-dependent transcripts [3]. As such, DDX3 was shown to directly interact with CRM1 in a NES- and RanGTP-independent manner [3]. The interaction between DDX3 and CRM1 was shown to occur at the cytoplasmic face of the nuclear pore complex suggesting that the RNA helicase was probably assisting the late cytoplasmic steps of nuclear export [3]. Several reports have also shown the involvement of DDX3 in translation of the HIV-1 unspliced mRNA [4–7]. During this process, the RNA helicase prepares the unspliced mRNA for translation initiation by acting on the TAR RNA motif [6,7]. As such, destabilization of TAR is essential for cap structure recognition by the eIF4F complex and the subsequent recruitment of the 40S ribosomal subunit [6]. Interestingly, this process seems to occur in cytoplasmic granules defined as a pre-translation initiation intermediate in which the unspliced mRNA accumulates together with DDX3 and a subset of translation initiation factors including eIF4GI and PABPC1 [5].

Since DDX3 is an essential host factor required to promote nuclear export and translation of HIV-1 mRNAs [3,5–7], it represents an interesting potential therapeutic target aimed to avoid viral resistance [8–10]. However, DDX3 has been involved in several steps of RNA metabolism and therefore, associated with different physiological processes including cell cycle progression, innate immune response and cancer [1,2,11,12]. Therefore, a thorough understanding on the functions and mechanisms of action of DDX3 is critical for the development of novel and safer antiviral drugs targeting this enzyme.

DDX3 belongs to the DEAD-box family of proteins, ATP-dependent RNA helicases characterized by the presence of a highly conserved helicase core domain [13]. This catalytic core is composed of two RecA-like domains containing motifs involved in ATP binding/hydrolysis, RNA binding and helicase activity [14,15]. DEAD-box proteins also function as RNA clamps for the assembly of large macromolecular complexes [15]. Interestingly, DEAD-box proteins interact with RNA through the sugar backbone and thus, binding is rather unspecific [14,

* Corresponding author.
E-mail address: rsotorifo@med.uchile.cl (R. Soto-Rifo).
[1] These authors should be considered as joint first authors.

http://dx.doi.org/10.1016/j.bbagrm.2016.03.009
1874-9399/

15]. Despite the high conservation of the helicase core domain, the mode of RNA binding and the enzymatic activity, the 37 DEAD-box proteins described so far in humans are expected to perform specific, non-redundant, functions within the cell [15,16]. As such, it has been suggested that regions flanking the catalytic core, which are variable both in length and amino acid composition, could be involved in conferring

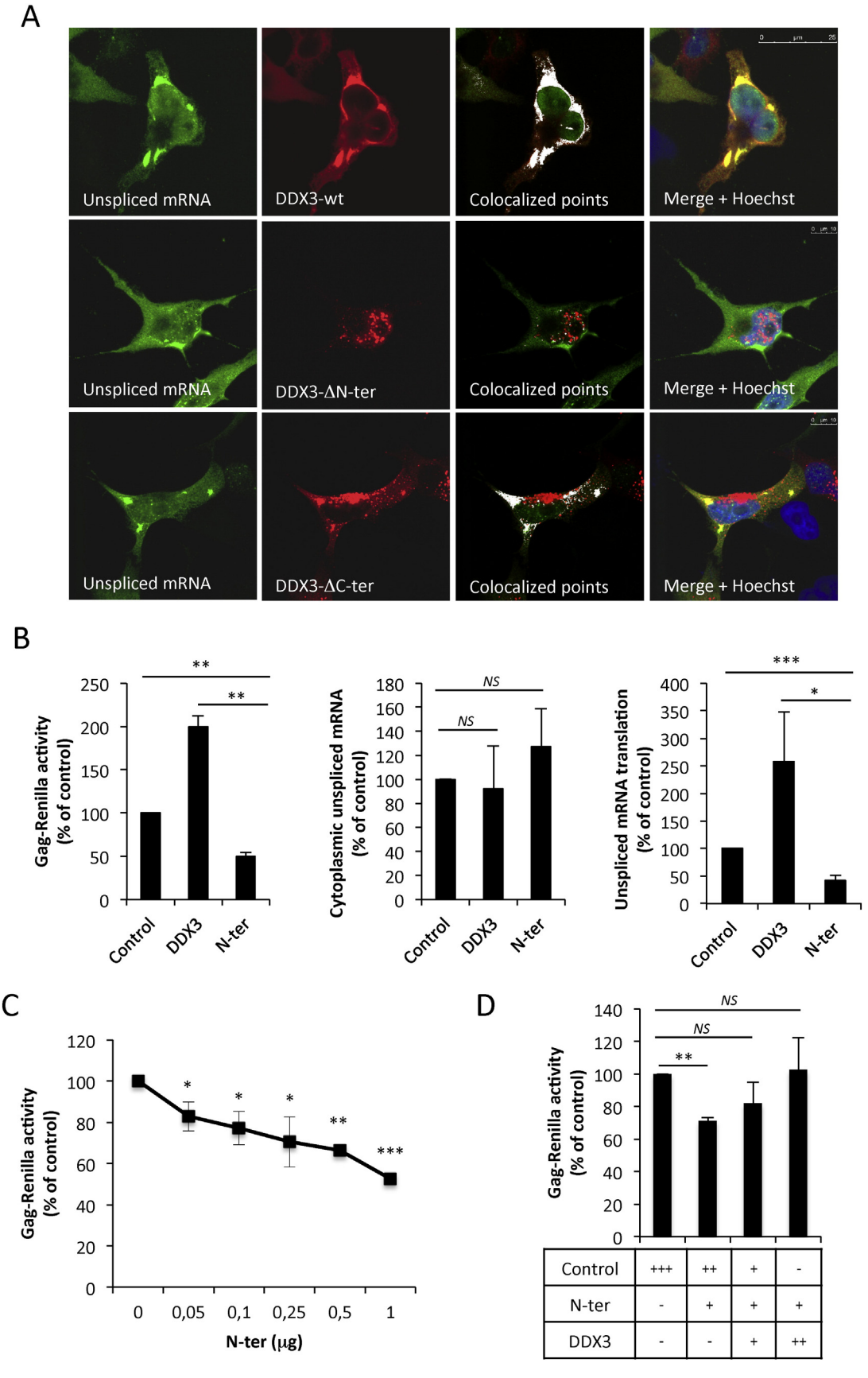

substrate specificity through the direct recruitment of protein co-factors or RNA partners [17].

Given the critical role of DDX3 as a host factor for HIV-1 Gag expression from the unspliced mRNA, we conducted a study aimed to determine the importance of the function of the N- and/or C-terminal domains of the RNA helicase in translation. By using cell imaging and functional assays with different reporter proviruses, we were able to identify the N-terminal domain of DDX3 as an important regulator of HIV-1 unspliced mRNA translation. Interestingly, our results suggest that DDX3 connects CRM1-dependent nuclear export with translation through its N-terminal extremity. These data reveal a novel mechanism that controls gene expression in HIV-1 and provide novel insights for the development of specific inhibitors.

2. Materials and methods

2.1. DNA constructs

The pNL4.3, pNL4.3R and pRod10R proviruses were previously described [18,19]. The pCMV-NL4.3R vector was obtained by replacing the FspAI/BssHII fragment by the CMV IE promoter amplified from the pCIneo vector (Promega). The pNL4.3RF vector was obtained by insertion of the *luc2* gene into the XhoI site of pNL4.3R. pCDNA HIV-1 5′-UTR and pCDNA β-globin 5′-UTR were constructed by inserting the corresponding region within a created HpaI site in pCDNA3.1 (Life Technologies). The pCIneo-HA-DDX3 was previously described [6] and was used as backbone to insert DDX3 ΔN-ter (183–662), DDX3 ΔC-ter (aa 1–540), DDX3 N-ter (aa 1–182), DDX3 N-ter (aa 22–182/ΔNES) and DDX3 N-ter Y38A/L43A at the EcoRI/NotI sites. pEGFP-CRM1 and pEGFP-Rev were constructed by inserting the CRM1 and Rev open reading frames into the pEGFP-C1 vector (Clontech) at the EcoRI site.

2.2. Cell culture and DNA transfection

HeLa cells were maintained in DMEM (Life Technologies) supplemented with 10% FBS (Hyclone) and antibiotics (Hyclone) at 37 °C and a 5% CO_2 atmosphere. Jurkat clone E6-1 [20], H9 T-lymphocytes [21] were maintained in RPMI 1640 (Life Technologies) supplemented with 10% FBS (Hyclone) and antibiotics (Hyclone) at 37 °C and a 5% CO_2 atmosphere. Cells were transfected using linear PEI ~25,000 Da (Polysciences) prepared as described previously [22]. HeLa cells were transfected using a ratio μg DNA/μl PEI of 1/10 and H9 cells were transfected using a ratio μg DNA/μl PEI of 1/15.

2.3. Virus production and infection

HEK293T cells were co-transfected with the pNL4.3-EGFP provirus and pVSVg together with either pCIneo-HA-d2EGFP or pCIneo-HA-N-ter as described above. Cell supernatants were collected at 96 hpt, cleared through a 0.22 μm filter and used to infect T-lymphocytes (Jurkat cells). At 48 hpi, EGFP-positive cells were analyzed through flow cytometry on a BD Accuri C6 Flow Cytometer and the BD Accuri CFlow software.

2.4. Analysis of cell viability

HeLa cells were transfected with pCIneo-HA-d2EGFP or pCIneo-HA-N-ter as described above and cell viability was analyzed through the incorporation of propidium iodide (1 μg/ml) by flow cytometry on a BD Accuri C6 Flow Cytometer and the BD Accuri CFlow software.

2.5. Analysis of Renilla and firefly activities

Renilla activity was determined using the *Renilla* Reporter Assay System (Promega) and *Renilla*/firefly activities were determined using the Dual Luciferase Reporter Assay System (Promega) in a GloMax® 96 microplate luminometer (Promega).

2.6. RNA extraction and RT-qPCR

Cytoplasmic RNA extraction and RT-qPCR from cytoplasmic RNA were performed as we have previously described [5]. Briefly, transfected cells were washed with PBS and recovered with PBS-EDTA 10 mM. Cells were pelleted at 3000 rpm for 5 min at 4 °C and lysed for 2 min at room temperature with 200 μl of buffer RLNa [10 mM Tris–HCl pH = 8.0, 10 mM NaCl, 3 mM $MgCl_2$, 1 mM DTT, 0.5% NP40 and 2 mM of vanadyl-ribonucleoside complex (VRC) (New England Biolabs)]. Cell lysates were centrifuged at 5000 rpm for 5 min at 4 °C and supernatant containing the cytoplasmic fraction was recovered and subjected to RNA extraction with TRIzol® Reagent (Life Technologies) as indicated by the manufacturer. Cytoplasmic RNAs (300 μg) were reverse-transcribed using the High Capacity RNA-to-cDNA Master Mix (Life Technologies) following the supplier's indications. For quantitative PCR, a 20-μl reaction mix was prepared with 5 μl of template cDNAs (previously diluted to 1/10), 10 μl of FastStart Universal SYBR Green Master (Rox) (Roche), 0.2 μM of sense and antisense primers and subjected to amplification using the Rotorgen fluorescence thermocycler (Qiagen). The GAPDH housekeeping gene was amplified in parallel to serve as a control reference. Relative copy numbers of *Renilla* luciferase cDNAs were compared to GAPDH using $x^{-\Delta Ct}$ (where x corresponds to the experimentally calculated amplification efficiency of each primer couple).

2.7. Fluorescent in situ hybridization, immunofluorescence and confocal microscopy

RNA FISH was carried out essentially as we recently described [5]. Briefly, HeLa cells were cultured in Lab-Tek™ Chamber Slides (Nunc™) and maintained and transfected with 0.5 μg of pNL4.3 and 0.2 μg of the corresponding HA vectors as indicated above. At 24 hpt, cells were washed twice with 1 × PBS and fixed for 10 min at room temperature with 4% paraformaldehyde at room temperature. Cells were

Fig. 1. The N-terminal domain of DDX3 is important for its incorporation into the HIV-1 unspliced mRNA ribonucleoprotein complex.

A) HeLa cells were transfected with 0.5 μg of pNL4.3 and 0.1 μg of pCIneo-HA-DDX3 (upper panels, scale bar 25 μm), pCIneo-HA-DDX3 ΔN-ter (middle panels, scale bar 10 μm) or pCIneo-HA-DDX3 ΔC-ter (lower panels, scale bar 10 μm). At 24 hpt cells were fixed and the unspliced mRNA (green) and HA-tag (red) were stained and analyzed by LS-CM. Colocalization points and merge plus Hoechst are also presented. Images presented are representative of several observed cells (>50 cells) obtained in at least two independent experiments.

B) HeLa cells were transfected with 0.3 μg of pNL4.3R and 1 μg of pCIneo-HA-d2EGFP (Control) or pCIneo-HA-N-ter. Gag synthesis (left panel), cytoplasmic unspliced mRNA (middle panel) and unspliced mRNA translation were determined at 24 hpt as indicated in the Materials and methods section. Experiments were performed in technical duplicates and results normalized to the control (arbitrary set to 100%) are presented as mean +/− SD of three independent experiments. (*$p < 0.05$; **$p < 0.01$; ***$p < 0.001$ and *NS*, non-significant).

C) HeLa cells were transfected with 0.3 μg of pNL4.3R and pCIneo-HA-d2EGFP (Control) or the indicated doses of pCIneo-HA-N-ter (pCIneo-HA-d2EGFP was used to transfect the same quantity of DNA). Gag synthesis was determined at 24 hpt as indicated in the Materials and methods section. Experiments were performed in technical duplicates and results normalized to the control (arbitrary set to 100%) are presented as mean +/− SD of three independent experiments. (*$p < 0.05$; **$p < 0.01$; ***$p < 0.001$).

D) HeLa cells were transfected with 0.3 μg of pNL4.3R and pCIneo-HA-d2EGFP (Control) or 1 μg of pCIneo-HA-N-ter and 0.5 μg (+) or 1 μg (++) of pCIneo-HA-DDX3 (pCIneo-HA-d2EGFP was used to transfect the same quantity of DNA). Gag synthesis was determined at 24 hpt as indicated in the Materials and methods section. Experiments were performed in technical duplicates and results normalized to the control (arbitrary set to 100%) are presented as mean +/− SD of three independent experiments. (**$p < 0.01$ and *NS*, non-significant).

subsequently permeabilized with 0.2% Triton X-100 for 5 min at room temperature and then hybridized overnight at 37 °C in 200 μl of hybridization mix (10% dextran sulfate, 2 mM VRC, 0.02% RNase-free BSA, 50% formamide, 300 μg tRNA and 120 ng of 11-digoxigenin-UTP probes) in a humid chamber. After hybridization, cells were washed with 0.2× SSC/50% formamide for 30 min at 50 °C and then incubated three times with antibody dilution buffer (2× SSC, 8% formamide, 2 mM vanadyl-ribonucleoside complex, 0.02% RNase-free BSA). Mouse anti-digoxin and rabbit anti-HA (Sigma Aldrich) primary antibodies diluted to 1/100 in antibody dilution buffer were added for 2 h at room temperature. Cells were washed 3 times with antibody dilution buffer and incubated with anti-mouse Alexa 488 and anti-rabbit Alexa 565 antibodies (Molecular Probes) diluted at 1/1000 for 90 min at room temperature. Cells were washed three times in wash buffer (2× SSC, 8% formamide, 2 mM vanadyl-ribonucleoside complex), twice with 1× PBS, incubated with Hoechst (Life Technologies) diluted to 1/10,000, for 5 min at room temperature, washed three times with 1× PBS, three times with water and mounted with Fluoromount (Life Technologies).

Images representative from several cells were obtained with a TCS SP5 AOBS Spectral Confocal Microscope (Leica Microsystems) and recovered and merged using the LAS AF Lite software (Leica Microsystems). Images were also obtained with an Olympus FluoView FV10i laser scanning confocal microscope (Olympus, USA; scale: 30 μm) and were analyzed using Imaris® software v.7.2.1 (Bitplane). Colocalized points were obtained using the colocalization analysis plug-in of ImageJ.

2.8. RNA immunoprecipitation

HEK293T cells growing in a 150 mm dish were co-transfected with pNL4.3 and pCIneo-HA-N-ter. At 24 hpt, cells were washed with PBS and crosslinked in 0.1% formaldehyde for 15 min at room temperature. Quenching buffer (2 M glycine; 25 mM Tris–HCl pH = 7.0) was added for 5 min at room temperature and cells were recovered at 400 ×g for 5 min. Cell pellets were resuspended in 300 μl of hypotonic lysis buffer (20 mM Tris–HCl pH 7.5, 15 mM NaCl, 10 mM EDTA, 0.5% NP-40, 0.1% Triton X-100, 2 mM VRC, 1× Protease inhibitor cocktail), sonicated and incubated on ice for 10 min. Volume was adjusted to 1 ml with hypotonic lysis buffer, NaCl was adjusted to 150 mM and extracts were incubated for 10 min on ice. Cell extracts were centrifuged at 10,000 ×g at 4 °C and the supernatant was pre-cleared and split into two. 10 μg of anti-HA antibody or IgG (Santa Cruz Biotechnologies) was added and the mix was incubated under rotation for 2 h at 4 °C. 50 μl of pre-washed Dynabeads Protein A magnetic beads (Life Technologies) was added and the mix was further incubated under rotation for 30 min at 4 °C. Protein–bead complex was recovered in a magnetic rack, washed 3 times with NET-2 buffer (20 mM Tris–HCl pH 7.5, 150 mM NaCl, 0.05% NP-40, 200 μM VRC, 1× Protease inhibitor cocktail). Immunoprecipitated material was treated with Proteinase K (New England Biolabs) and subjected to RNA extraction and RT-qPCR as indicated above.

2.9. Proximity ligation assay (PLA)

In situ PLA detection was carried out using the DUOLINK II In Situ kit (OLINK Bioscience) according to the protocol provided by the manufacturer. Briefly, cells expressing EGFP-CRM1 and HA-tagged DDX3 or N-ter were blocked with 1× blocking solution (Roche) at 37 °C for 30 min. Primary antibodies (mouse anti-HA 1/250 and rabbit anti-GFP

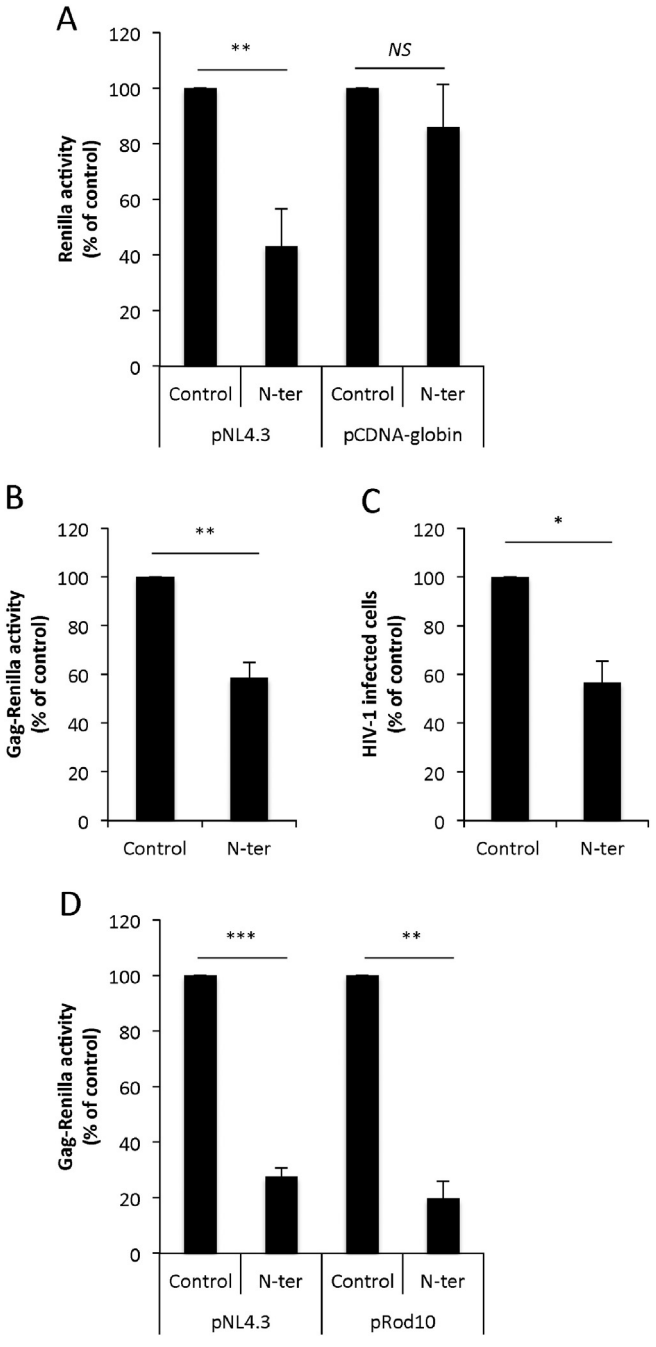

Fig. 2. N-ter interferes specifically with HIV-1 and HIV-2 gene expression.

A) HeLa cells were transfected with 0.3 μg of pNL4.3R or 0.3 μg of pCDNA-globin DNA together with 1 μg of pCIneo-HA-d2EGFP (Control) or pCIneo-HA-N-ter. Protein synthesis was determined at 24 hpt as indicated in the Materials and methods section. Experiments were performed in technical duplicates and results normalized to the control (arbitrary set to 100%) are presented as mean +/− SD of three independent experiments. (**$p < 0.05$, *NS*, non-significant).

B) H9 T-lymphocytes were transfected with 0.3 μg of pNL4.3R together with 0.1 μg pCMV-Firefly and 1 μg of pCIneo-HA-d2EGFP (Control) or pCIneo-HA-N-ter. Gag and Firefly synthesis was determined at 24 hpt as indicated in the Materials and methods section. Experiments were performed in technical duplicates and the Gag/Firefly ratios normalized to the control (arbitrary set to 100%) are presented as mean +/− SD of three independent experiments. (**$p < 0.01$).

C) HEK293T cells were transfected with pNL4.3-EGFP, pVSVg and pCIneo-HA-d2EGFP (Control) or pCIneo-HA-N-ter. At 96 hpt, supernatants containing pseudotyped virus were used to infect Jurkat cells. HIV-1-infected cells were analyzed by FACS analyses as described in the Materials and methods section. Experiments were performed in technical duplicates and results normalized to the control (arbitrary set to 100%) are presented as mean +/− SD of three independent experiments. (*$p < 0.05$).

D) HeLa cells were transfected with 0.3 μg of pNL4.3R or 0.3 μg of pRod10R together with 1 μg of pCIneo-HA-d2EGFP (Control) or pCIneo-HA-N-ter. Gag synthesis was determined at 48 hpt as indicated in the Materials and methods section. Experiments were performed in technical duplicates and results normalized to the control (arbitrary set to 100%) are presented as mean +/− SD of three independent experiments (**$p < 0.01$ and ***$p < 0.001$).

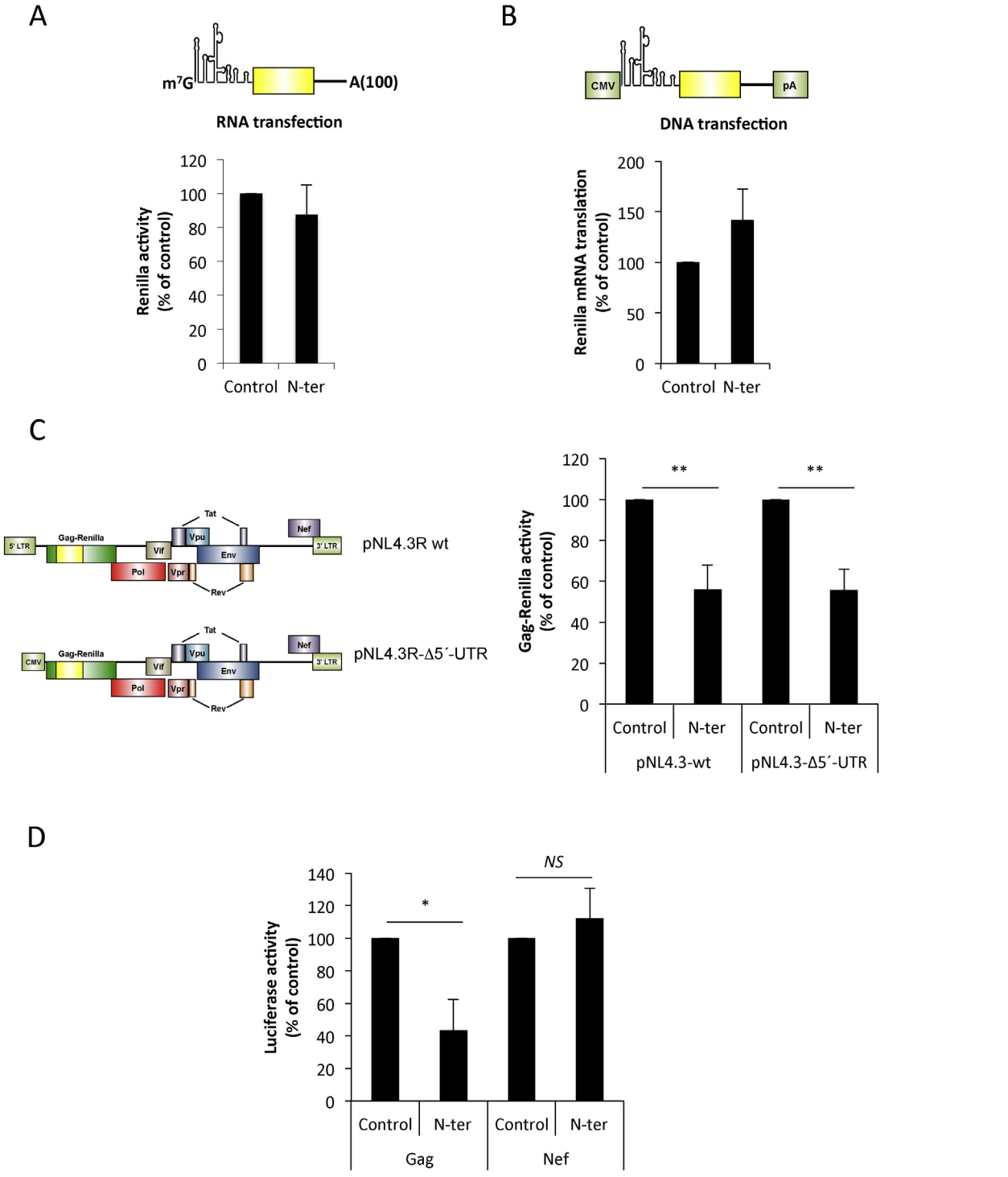

Fig. 3. N-ter interferes specifically with the unspliced mRNA in the context of a full-length provirus.

A) HeLa cells were transfected with 1 μg of pCIneo-HA-d2EGFP (Control) or pCIneo-HA-N-ter for 24 h and then transfected with 0.3 μg of pRenilla-5′-UTR. *Renilla* synthesis was determined at 3 hpt as indicated in the Materials and methods section. Experiments were performed in technical duplicates and results normalized to the control (arbitrary set to 100%) are presented as mean +/− SD of three independent experiments.

B) HeLa cells were transfected with 0.3 μg of pCDNA-HIV-1 DNA and 1 μg of pCIneo-HA-d2EGFP (Control) or pCIneo-HA-N-ter. *Renilla* synthesis was determined at 24 hpt as indicated in the Materials and methods section. Experiments were performed in technical duplicates and results normalized to the control (arbitrary set to 100%) are presented as mean +/− SD of three independent experiments.

C) HeLa cells were transfected with 0.3 μg of pNL4.3R or 0.3 μg of pNL4.3R-Δ5′-UTR (see cartoons) together with 1 μg of pCIneo-HA-d2EGFP (Control) or pCIneo-HA-N-ter. Gag synthesis was determined at 24 hpt as indicated in the Materials and methods section. Experiments were performed in technical duplicates and results normalized to the control (arbitrary set to 100%) are presented as mean +/− SD of three independent experiments (**$p < 0.01$).

D) HeLa cells were transfected with 0.3 μg of pNL4.3RF and 1 μg of pCIneo-HA-d2EGFP (Control) or pCIneo-HA-N-ter. Protein synthesis was determined at 24 hpt as indicated in the Materials and methods section. Experiments were performed in technical duplicates and results normalized to the control (arbitrary set to 100%) are presented as mean +/− SD of three independent experiments (*$p < 0.05$).

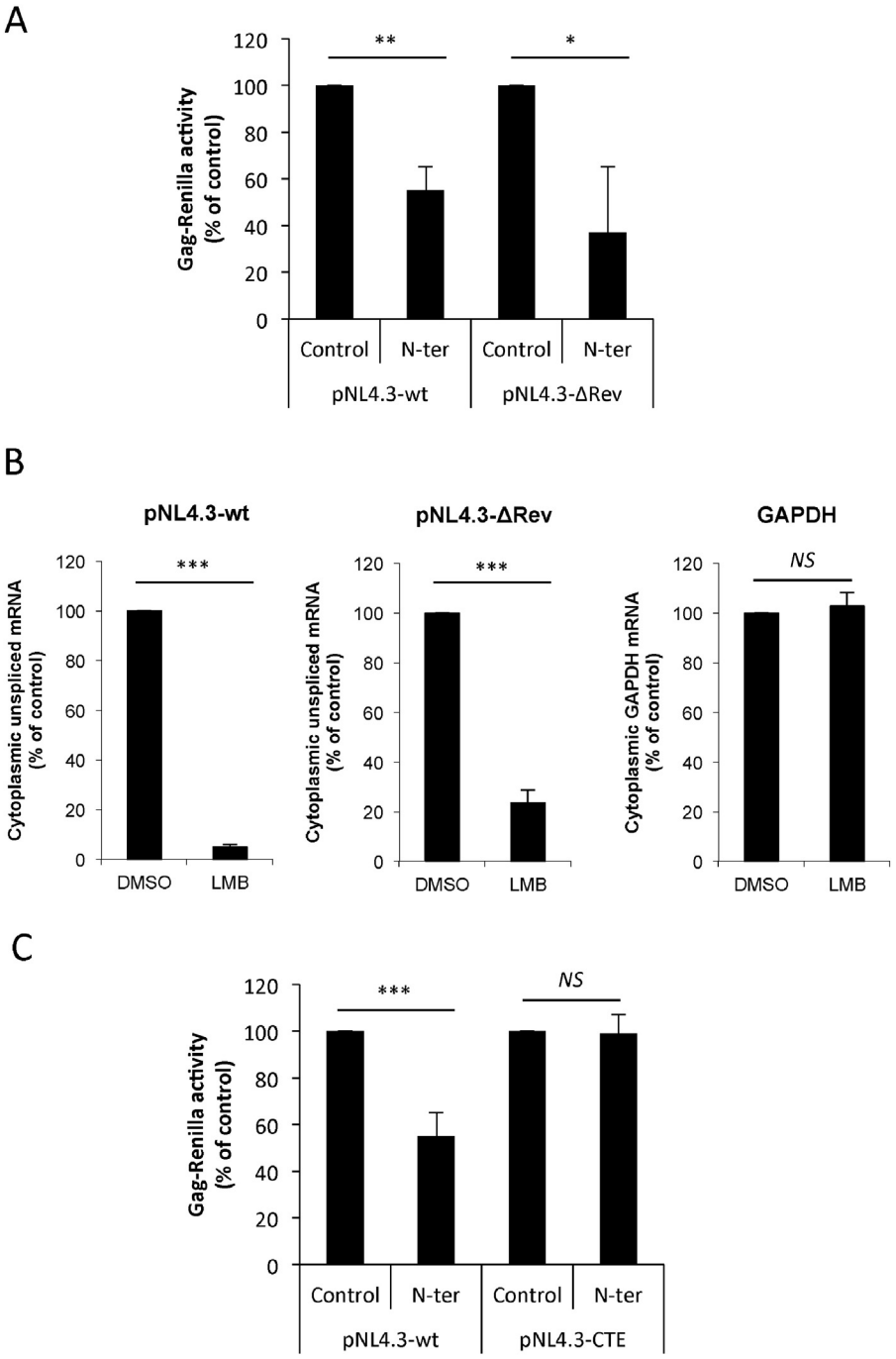

Fig. 4. DDX3 connects nuclear export with translation of the HIV-1 unspliced mRNA.

A) HeLa cells were transfected with 0.3 μg of pNL4.3R or 0.3 μg of pNL4.3R-ΔRev together with 1 μg of pCIneo-HA-d2EGFP (Control) or pCIneo-HA-N-ter. Gag synthesis was determined at 24 hpt as indicated in the Materials and methods section. Experiments were performed in technical duplicates and results normalized to the control (arbitrary set to 100%) are presented as mean +/− SD of three independent experiments (*$p < 0.05$).

B) HeLa cells were transfected with 0.3 μg of pNL4.3R or 0.3 μg of pNL4.3R-ΔRev and treated with 20 nM of Leptomycin B (LMB). The indicated cytoplasmic mRNAs were quantified at 24 hpt as indicated in the Materials and methods section. Experiments were performed in technical duplicates and results normalized to the control (arbitrary set to 100%) are presented as mean +/− SD of three independent experiments (***$p < 0.001$).

C) HeLa cells were transfected with 0.3 μg of pNL4.3R or 0.3 μg of pNL4.3R-CTE together with 1 μg of pCIneo-HA-d2EGFP (Control) or pCIneo-HA-N-ter. Gag synthesis was determined at 24 hpt as indicated in the Materials and methods. Experiments were performed in technical duplicates and results normalized to the control (arbitrary set to 100%) are presented as mean +/− SD of three independent experiments (***$p < 0.001$).

1/250 from Santa Cruz Biotechnologies) were added and then incubated for 1 h at 37 °C. Slides were washed twice with Wash Buffer A for 5 min each, then secondary antibodies (DUOLINK anti-rabbit PLA-plus probe, DUOLINK anti-mouse PLA-minus probe) were added and incubated at 37 °C for 1 h. Upon two washes with Wash Buffer A ligation mix was added, incubated at 37 °C for 30 min and washed again twice with Wash Buffer A. Amplification reaction was carried out at 37 °C for 100 min. Subsequently, slides were washed twice with Wash Buffer B and mounted with Duolink® In Situ Mounting Medium with DAPI. Images were acquired using an Olympus FluoView FV10i laser scanning

confocal microscope (Olympus, USA; scale: 30 μm) and were analyzed and obtained using Imaris® software v.7.2.1 (Bitplane). Dots were counted using Imaris® software v.7.6 (Bitplane) using a 0.5 μm diameter measure for negative condition and 0.1 μm for DDX3 and N-ter. Effectively transfected cells were identified using Imaris® software using GFP intensity of cells.

2.10. In silico predictions

RNA-binding predictions were performed with the BindN and RNAbindR software [23,24]. In order to predict intrinsically disordered regions in DDX3 we used IUPred [25] and the disorder tendency score was plotted in a heat map. To predict intrinsically disordered regions of human DEAD-box helicase proteins, sequences at the RNA helicase database [16] were analyzed with the MeDorv1.4 metaserver, which run different predictors at the same time [26]. We obtained results from four different software (IUPred, GlobPlot2 [27], DisEMBL [28] and FoldIndex [29]) and we considered an amino acid in an intrinsically disordered region only if at least two of the four software predicted it to be disordered.

3. Results

3.1. The N-terminal domain of DDX3 is required for HIV-1 unspliced mRNA translation

Our previous studies identified DDX3 as a host factor essential for HIV-1 unspliced mRNA translation [5,6]. We also showed that DDX3 drives the ATP-dependent assembly of cytoplasmic granules, which we defined as a pre-translation initiation intermediate required for the unspliced mRNA to recruit the 43S initiation complex onto the 5′ end cap structure [5]. In order to investigate whether the N- and/or C-terminal domains of DDX3 are involved in this process, we used the ability of DDX3 to drive the assembly of cytoplasmic granules together with the viral mRNA as an indicator of its function. Thus, we performed RNA FISH and immunofluorescence on cells expressing HIV-1 NL4.3 together with HA-tagged wild type or mutant versions of DDX3 and look for the assembly of pre-translation initiation intermediates by LS-CM (Fig. 1A). While co-localization of the unspliced mRNA and DDX3 in cytoplasmic granules was readily observed when using the wild type and the ΔC-terminal mutant of DDX3 (Fig. 1A, upper and bottom panels), this phenotype was not observed when a mutant of DDX3 lacking the N-terminal domain was used (Fig. 1A, middle panels). Indeed, while the wild type and ΔC-terminal versions of DDX3 presented a rather cytoplasmic localization either in the presence or absence of HIV-1, the ΔN-ter was confined to the nucleus (Fig. 1A and data not shown). These data suggest that the N-terminal domain of DDX3 is required for the incorporation of the protein into the viral mRNP and its co-localization with the unspliced mRNA in cytoplasmic granules. In agreement with this, the mutant protein lacking the N-terminal domain was not able to stimulate unspliced mRNA translation when overexpressed (Supplementary Fig. 1A), suggesting a correlation between the incorporation of the protein into the viral mRNP and its ability to stimulate translation. In order to further characterize the involvement of the N-terminal domain of DDX3 on Gag expression from the unspliced mRNA, we overexpressed the isolated domain observing a 2-fold inhibition in protein synthesis (Fig. 1B, left panel). Of note, N-ter overexpression affected Gag synthesis without altering the cytoplasmic accumulation of the unspliced mRNA suggesting an effect on translation (Fig. 1B, middle and right panels). It should be mentioned that this effect of N-ter overexpression on unspliced mRNA translation was identical to that observed when the dominant negative mutant DDX3^{DQAD} was overexpressed (Supplementary Fig. 1B). In addition, the effect of N-ter on gene expression from the HIV-1 unspliced mRNA was not due to any effect on cell viability as evidenced by propidium iodide incorporation in control and N-ter-expressing cells (Supplementary Fig. 1C).

We then used the BindN and RNAbindR software to predict RNA binding residues in N-ter [23,24]. From these in silico predictions, we identify three clusters of residues forming putative RNA binding domains (RBD, Supplementary Fig. 1D). We selected residues presenting the best scores in each RBD to perform site-directed mutagenesis and analyze their contribution to N-ter function (Supplementary Table 1). However, all RBD mutants analyzed inhibited Gag expression at the same extent as wild type N-ter raising the possibility that N-ter is not involved in unspliced mRNA binding (Supplementary Fig. 1D). Consisting with this idea, RNA-immunoprecipitation analyses revealed that the unspliced mRNA is marginally enriched in the N-ter immunoprecipitated fraction (Supplementary Fig. 1E). Interestingly, we observed that the inhibitory effect of N-ter was dose-dependent (Fig. 1C) and reversed by co-expression of full-length DDX3 (Fig. 1D) indicating that N-ter somehow interferes with the recruitment of the endogenous protein onto the viral mRNP. Together, these data indicate that the N-terminal domain of DDX3 allows its incorporation into the viral mRNP but is not sufficient for translational activation.

3.2. N-ter interferes with a specific step of HIV-1 gene expression that is conserved in HIV-2

Having determined that overexpression of N-ter blocks HIV-1 Gag expression by interfering with unspliced mRNA translation, we then sought to determine whether such an effect was specific for HIV-1. For this, we analyzed the effect of overexpressing N-ter on gene expression from a *Renilla* luciferase expressing plasmid (Fig. 2A). As observed, N-ter inhibited specifically Gag synthesis from the unspliced mRNA without affecting *Renilla* synthesis from the reporter plasmid. Such a reduction in Gag synthesis was also observed in CD4 + T-lymphocytes (Fig. 2B) and has a direct impact in virus production as evidenced in infection assays in Jurkat cells using pseudotyped viruses produced from control and N-ter-expressing cells (Fig. 2C).

We were also interested in determining whether such an effect of N-ter was conserved in the closely related human lentivirus HIV-2 (Fig. 2D). For this, we used a HIV-2 Rod10-derived proviral DNA that carries the *Renilla* luciferase ORF inserted within the *gag* gene [19]. Similar to what was observed with HIV-1, N-ter was also able to interfere with Gag synthesis from the HIV-2 unspliced mRNA indicating that the mechanism of action of DDX3 is conserved in both human lentiviruses.

3.3. The N-terminal domain of DDX3 acts upstream remodeling of the 5′-UTR

Given the apparent specificity of inhibition of N-ter during HIV-1 unspliced mRNA translation, we were mostly interested in the mechanism by which this occurs in order to better characterize the function of DDX3 during HIV-1 gene expression. As previous studies showed that DDX3 was required to promote translation by acting on the 5′-untranslated region (5′-UTR) of the HIV-1 unspliced mRNA [4,6,7], we sought to determine whether N-ter was interfering with ribosome recruitment onto the 5′-UTR (Fig. 3). For this, we first transfected cells expressing N-ter with a capped and polyadenylated in vitro-transcribed reporter mRNA in which *Renilla* luciferase synthesis was driven by the HIV-1 unspliced mRNA 5′-UTR (Fig. 3A). However, we observed that N-ter was not able to block *Renilla* luciferase synthesis suggesting that N-ter was not targeting the remodeling of the 5′-UTR. As it could be argued that nuclear experience is important for N-ter to interact with the viral 5′-UTR, we also analyzed the effect of N-ter on HIV-1 5′-UTR-driven *Renilla* luciferase expression from a plasmid DNA but observed the same inability to block reporter gene synthesis (Fig. 3B). Thus, it seems that N-ter only exerts its effects in the context of a proviral DNA suggesting that N-ter could be blocking unspliced mRNA translation by acting

upstream the remodeling of the 5′-UTR. To test such a hypothesis, we generated a proviral DNA in which the viral promoter and most of the 5′-UTR were deleted and replaced by the CMV IE promoter (see scheme in Fig. 3C and the Materials and methods section for details). Analysis of Gag expression from the wild type and Δ5′-UTR proviral DNAs revealed that N-ter was effectively interfering with translation independently of the 5′-UTR (Fig. 3C).

Given the fact that the TAR RNA motif was identified as the main target of DDX3 during translation [6,7] and such RNA motif is present in all HIV-1 transcripts [30], we then sought to determine whether N-ter was

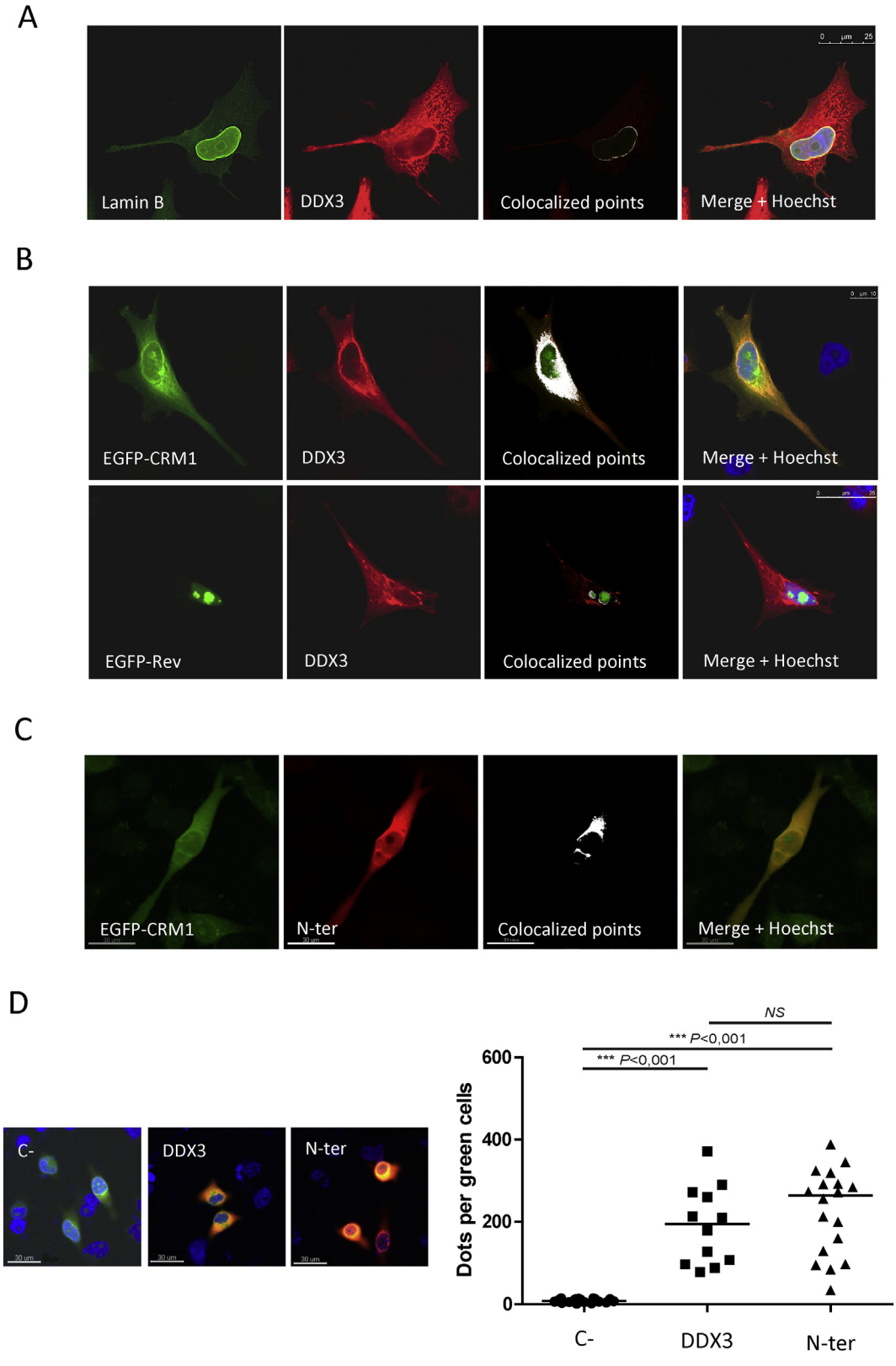

interfering with a process that is common to other viral mRNAs. For this, we generated a dual reporter provirus by inserting the Firefly luciferase reporter gene within the *nef* gene of the pNL4.3R vector [19]. Interestingly, we observed that expression of N-ter interfered with Gag synthesis without affecting Nef expression (Fig. 3D), indicating that inhibition by N-ter is specific for the unspliced mRNA.

3.4. The N-terminal domain of DDX3 connects translation with CRM1-dependent nuclear export

Results presented above indicate that protein synthesis from the fully spliced Nef mRNA is not affected by N-ter while Gag expression from the unspliced mRNA is specifically blocked. Since DDX3 was proposed to act as a co-factor of the viral protein Rev during nuclear export [3], we wanted to determine whether inhibition by N-ter was linked to Rev function. For this, we analyzed the effect of N-ter on Gag synthesis from the wild type and ΔRev proviruses. Interestingly, we observed that N-ter interfered with protein synthesis from the unspliced mRNA regardless of the presence or absence of Rev (Fig. 4A). This observation is in agreement with our previous data showing that siRNA-mediated knockdown of DDX3 also inhibited unspliced mRNA translation from the ΔRev provirus [5] and suggests that the function of DDX3 on translation is uncoupled from Rev activity. Indeed, to our knowledge there is no experimental evidence showing a direct interaction between DDX3 and Rev and the RNA helicase was rather shown to directly contact CRM1 in a NES- and RanGTP-independent manner [3]. Thus, it is possible that DDX3 would be coupling unspliced mRNA translation with CRM1-dependent nuclear export through its N-terminal domain. As a first approach to validate this hypothesis, we measured the amount of unspliced mRNA that is exported by CRM1 to the cytoplasm in the absence of Rev. For this, we quantified the cytoplasmic unspliced mRNA produced by wild type and ΔRev proviruses in the presence or absence of Leptomycin B (LMB), a potent inhibitor of CRM1-dependent nuclear export known to block cytoplasmic accumulation of the HIV-1 unspliced mRNA [31]. As it could be expected, the cytoplasmic accumulation of the unspliced mRNA was reduced by 3.5-fold in the absence of Rev (Supplementary Fig. 2). We also observed that cytoplasmic accumulation of the unspliced mRNA but not GAPDH mRNA was dramatically reduced in the presence of 20 nM of LMB (Fig. 4B). Interestingly, cytoplasmic accumulation of the unspliced mRNA was also diminished by LMB in the absence of Rev indicating that the extent of nuclear export of this viral mRNA occurred through the CRM1 pathway (Fig. 4B). Thus, if the blockade of translation exerted by the N-ter requires the CRM1-dependent nuclear export of the unspliced mRNA, one could expect that replacing the nuclear export pathway would abolish this effect. In order to confirm this assumption, we analyzed the effects of N-ter expression on the pNL4.3-RRE(−)Rev(−)-CTE(+) provirus [32]. This provirus lacks the Rev responsive Element (RRE) and Rev but contains the Constitutive Transport Element from the Simian Retrovirus 1, which allows nuclear export through the NXF1-dependent pathway [33]. Thus, we inserted the *Renilla* luciferase reporter gene into the *gag* gene of pNL4.3-RRE(−)Rev(−)CTE(+) provirus as described [19] and analyzed the effect of N-ter on Gag synthesis from the unspliced mRNA. As observed above, N-ter interfered with gene expression from the unspliced mRNA in the context of the wild type provirus (Fig. 4C, see pNL4.3-wt). However, the unspliced mRNA generated from the pNL4.3-RRE(−)Rev(−)CTE(+) provirus and thus, exported through the NXF1 pathway was unaffected (Fig. 4C, see pNL4.3-CTE), confirming that the N-terminal domain allows the RNA helicase to connect CRM1-dependent nuclear export with translation of the unspliced mRNA.

3.5. DDX3 interacts with CRM1 at the nuclear envelope and the cytoplasm through the N-terminal domain

As results presented above indicate that DDX3 is linking nuclear export and translation of the unspliced mRNA through CRM1 independently of Rev function, we wanted to visualize the DDX3–CRM1 complex by LS-CM (Fig. 5). DDX3 localizes preferentially in the cytoplasm but also concentrates at the nuclear envelope where it co-localizes with the marker Lamin B (Fig. 5A). Consistent with previous reports [3] and data presented above, DDX3 co-localizes with CRM1 both at the nuclear envelope and in the cytoplasm (Fig. 5B, upper panels) further confirming that DDX3 may contact the HIV-1 unspliced mRNP through its interactions with the nuclear export factor. In sharp contrast, we were not able to detect co-localization between DDX3 and Rev (Fig. 5B, lower panels) although an unspliced mRNA-dependent interaction could not be discarded.

We then analyzed whether the DDX3-CRM1 co-localization observed above was recapitulated with N-ter. Similar to what was obtained with DDX3, we observed a strong co-localization between CRM1 and N-ter at the nuclear periphery and the cytoplasm suggesting that DDX3 reaches CRM1 through its N-terminal domain (Fig. 5C). To further confirm this idea, we carried out a proximity ligation assay (PLA) in order to observe and quantify individual protein–protein complexes in cells [34]. In this assay, a single CRM1/DDX3 or CRM1/N-ter complex can be observed as a red dot only if both proteins are in close proximity (Fig. 5D). As observed, PLA signal was observed with both CRM1/DDX3 and CRM1/N-ter but not the negative control further indicating that DDX3 and CRM1 are components of the same complex (Fig. 5D, compare C- with DDX3 and N-ter). Dots/cell quantification revealed no significant differences between DDX3 and N-ter suggesting that the N-terminal domain of DDX3 is important for its interaction with CRM1 (Fig. 5D, see panel on the right).

3.6. Intrinsic disorder is characteristic of the N- and C-terminal domains of human DEAD-box proteins

We finally sought to gain insights into the properties of N-ter that could be relevant for DDX3 functions. Indeed, previous reports have identified different features and functions within the N-terminal domain of DDX3. These include the region spanning residues 11–21 showed to contain a leucine-rich NES [3], residues 11–90 necessary for Vaccinia Virus K7 interaction [35], residues 38–43 involved in eIF4E binding and stress granules assembly [36,37], residues 135–166 which contain an ATP binding loop critical for RNA-stimulated ATPase activity [11] or Ser102, whose phosphorylation by TBK1 is required for interaction with IRF3 [38]. From these key features, those that could be related to the functions of N-ter in connecting nuclear export and translation of

Fig. 5. DDX3 localizes with CRM1 through the N-terminal domain.

A) HeLa cells were transfected with 0.1 μg of pCIneo-HA-DDX3. At 24 hpt cells were fixed and the HA-tag (red) and endogenous Lamin B (green) were stained and analyzed by LS-CM. Colocalization points and merge plus Hoechst are also presented. Scale bar 25 μm.

B) HeLa cells were transfected with 0.1 μg of pCIneo-HA-DDX3 and 0.1 μg of pEGFP-CRM1 (upper panels) or pEGFP-Rev (bottom panels). At 24 hpt cells were fixed and the HA-tag (red) was stained and analyzed together with EGFP (green) by LS-CM. Colocalization points and merge plus Hoechst are also presented. Scale bar 10 μm (upper) and 25 μm (bottom).

C) HeLa cells were transfected with 0.1 μg of pCIneo-HA-N-ter and 0.1 μg of pEGFP-CRM1. At 24 hpt cells were fixed and the HA-tag (red) was stained and analyzed together with EGFP (green) by LS-CM. Colocalization points and merge plus Hoechst are also presented. Scale bar 30 μm.

D) HeLa cells were transfected with 0.1 μg of pEGFP-CRM1 together with 0.1 μg of pCIneo-HA-DDX3 or pCIneo-HA-N-ter and subjected to PLA using rabbit anti-GFP antibody and the Duolink® in situ kit (negative control, C-) or rabbit anti-GFP antibody together with mouse anti-HA antibody and the Duolink® in situ kit (DDX3 and N-ter). Representative images are presented as the merge of EGFP-CRM1 (green) and PLA (red). Dots per green cells are presented in C- (n = 20 cells), DDX3 (n = 12 cells) and N-ter (n = 18 cells) (*NS* = non-significant).

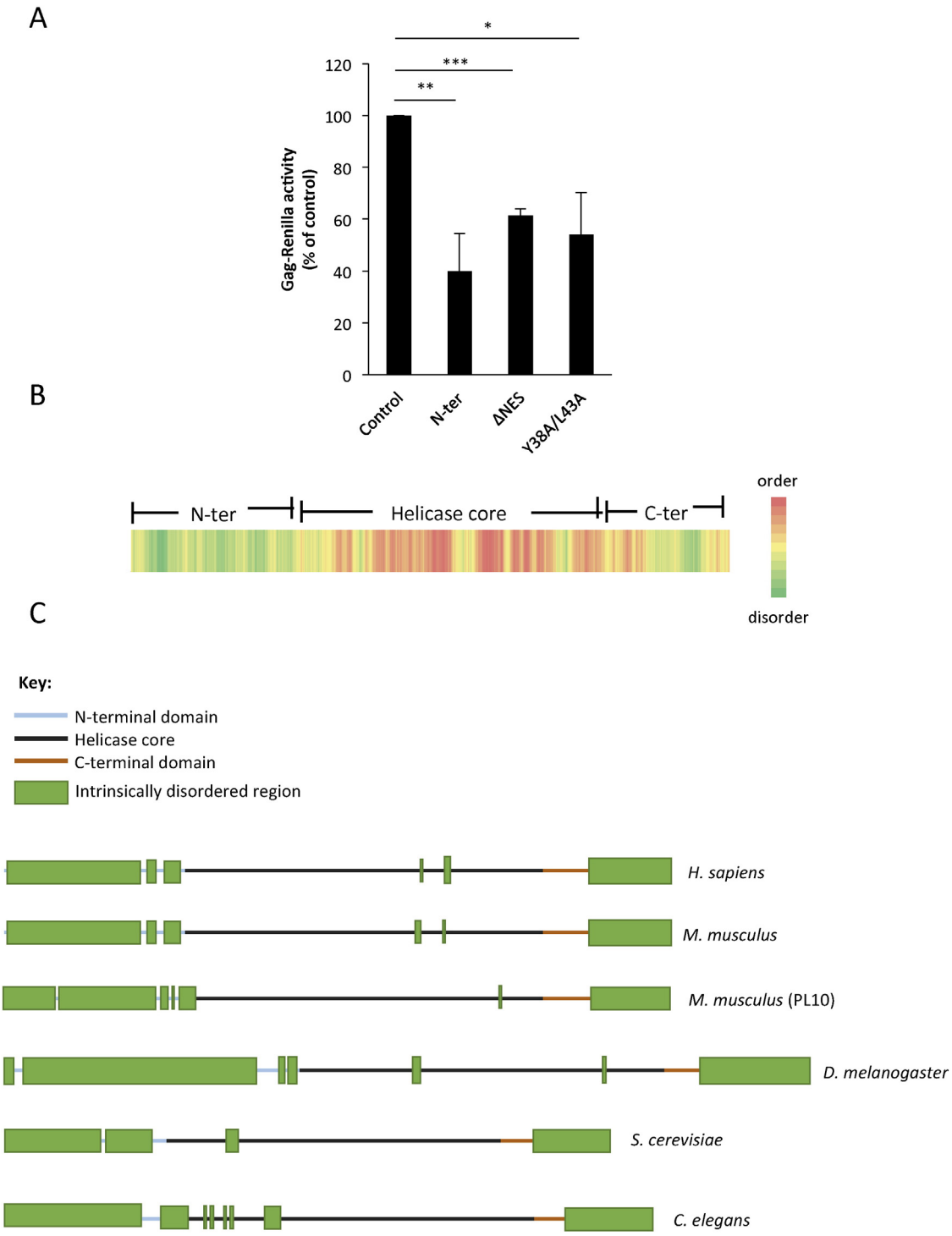

Fig. 6. The N-terminal domain of DDX3 is intrinsically disordered.

A) HeLa cells were transfected with 0.3 μg of pNL4.3R and 1 μg of pCIneo-HA-d2EGFP (Control), pCIneo-HA-N-ter, pCIneo-HA-N-ter ΔNES or pCIneo-HA-N-ter Y38A/L43A. Gag synthesis was determined at 24 hpt as indicated in the Materials and methods section. Experiments were performed in technical duplicates and results normalized to the control (arbitrary set to 100%) are presented as mean +/− SD of three independent experiments (*$p < 0.05$; **$p < 0.01$ and ***$p < 0.001$).

B) Intrinsic disorder of the human DDX3 sequence was analyzed with IUPred and is represented as heat map.

C) Schematic representation of intrinsically disordered regions in Human DDX3 and its mouse, fruit fly, yeast and nematode homologs. Sequences were analyzed with MeDorv1.4 metaserver as described in the Materials and methods section. Data summarized in Table 1 are schematically represented in the figure.

the HIV-1 unspliced mRNA are the leucine-rich NES and the YxxxxLϕ eIF4E-binding domain. Thus, we analyzed the effect of N-ter lacking the leucine-rich NES (ΔNES) or carrying the Y38A/L43A mutations (Fig. 6A). However, these mutants showed similar inhibitory activities as wild type N-ter indicating that the effect observed does not rely on these features and other to-be-determined features are involved in N-ter function.

Interestingly, circular dichroism data suggested that the N-terminal region of DDX3 is unstructured [35], a typical feature of intrinsically disordered regions in proteins [39]. As such, in silico predictions revealed

Table 1
Intrinsically disordered regions in DDX3X homologs.

Specie	Protein	Intrinsically disordered regions[a]	Access number (Uniprot)
H. sapiens	DDX3X	19–151 (N), 154–163 (N), 165–181 (N); 472–473 (H), 479–483 (H); 580–662 (C)	O00571
M. musculus	DDX3X	19–151 (N), 154–163 (N), 165–181 (N), 472–473 (H), 483, 581–662 (C)	Q62167
	PL10	1–51 (N), 54–150 (N), 153–160 (N), 161–162 (N), 164–180 (N–H), 471–472 (H), 579–660 (C)	P16381
D. melanogaster	Belle	1–10 (N), 20–254 (N), 277–283 (N), 285–294 (N), 364–372 (H), 590–593 (H), 685–798 (C)	Q9VHP0
S. cerevisiae	Ded1p	1–95 (N), 99–145 (N), 206–218 (H), 528–604 (C)	P06634
C. elegans	Y71H2AM.19	1–137 (N), 148–175 (N–H), 187–188 (H), 192–194 (H), 206 (H), 208 (H), 235–251 (H)	Q4W5R4

[a] (N) = N-terminal domain; (H) = helicase core; (C) = C-terminal domain.

that both the N-terminal and C-terminal domains of DDX3 are enriched in intrinsically disordered regions when compared to the catalytic helicase core (Fig. 6B), which is mainly composed by structured domains conserved amongst DEAD-box proteins [40]. The enrichment in intrinsically disordered regions in domains flanking the helicase core was not only observed in the mouse, yeast, fly and worm homologs of human DDX3 (Fig. 6C and Table 1) but also in all human DEAD-box proteins described in the RNA helicase database [16] (Supplementary Table 2). These data further indicate that the presence of intrinsically disordered regions may be important for substrate specificity and RNA helicase function.

4. Discussion

DDX3 is a host factor essential for HIV-1 replication as evidenced by several reports including different genome-wide siRNA screenings [1,41]. During viral replication, DDX3 was shown to promote nuclear export and translation of the unspliced mRNA. To do so, the RNA helicase interacts with: i) the viral mRNA, ii) the karyopherin CRM1 and iii) translation initiation factors eIF4GI and PABPC1 [3,6]. However, whether these two activities of DDX3 during the post-transcriptional control of HIV-1 gene expression are interconnected or independent has never been evaluated.

In this work we first show that the N-terminal domain of DDX3 (amino acids 1–182) regulates the functions of this RNA helicase during HIV-1 unspliced mRNA translation (Figs. 1 and 2). Given the fact that N-ter inhibits unspliced mRNA translation in a CRM1-dependent but 5′-UTR-independent manner, our data suggest that N-ter could be involved in a step of gene expression occurring after nuclear export but before the 40S ribosomal subunit is recruited onto the viral 5′-UTR (Fig. 3). In agreement with this idea, we observed that the regulatory effect of the N-terminal domain of DDX3 was independent of Rev but rather relied on nuclear export by CRM1 (Figs. 4 and 5). Consistent with this data, a recent docking study aimed to characterize the human DDX3–CRM1–NES–RanGTP multimeric complex proposed an interesting mode of binding between regions present in the helicase domain of DDX3 and a region surrounding to the NES-binding pocket of CRM1 [42]. Such a binding was stimulated by the binding of RanGTP to CRM1 but was independent of the NES-containing cargo [42]. Unfortunately, there is no structural data of the full-length DDX3 and thus, the abovementioned simulations were performed in the absence of the N-terminal domain that we showed as an important determinant for interaction with CRM1 (Fig. 5). Indeed, our data suggest that DDX3 is incorporated into the CRM1-nuclear export viral mRNP through the N-terminal domain to promote viral mRNA translation. As such, the isolated N-terminal domain of DDX3 interferes with the recruitment of the full-length protein into this complex. Of note, our previous and present data indicate that DDX3 promotes HIV-1 gene expression independently of the viral protein Rev (Fig. 4) [5]. These observations suggest that DDX3 is recruited onto the exported viral mRNP to play its functions most probably once Rev has been released from the complex.

Interestingly, it was recently reported that the formation of a Ded1–CRM1–RanGTP trimeric complex in yeast resulted in a reduced RNA-stimulated ATPase activity of Ded1 [43]. This phenomenon was dependent on the NES present in Ded1 and occurred concomitantly with the increase in the Km for the RNA substrate suggesting that the NES-dependent interaction between Ded1 and CRM1–RanGTP may modulate substrate specificity of the RNA helicase [43]. Although the interaction between human DDX3 and CRM1 seems not to rely on a NES [3], it would be interesting to determine whether such a modulation of the enzymatic activity of DDX3 also occurs in the presence of the RRE/Rev–CRM1–RanGTP complex. Thus, it is tempting to speculate that DDX3 (and Ded1) could be acting on the CRM1-dependent pathway analogously to Dbp5 in the NXF1-dependent nuclear export pathway [44].

As suggested by previous data [45], we identified that the N-terminal and C-terminal domains of DDX3 were enriched in intrinsically disordered regions (Fig. 6). We also found that this characteristic was conserved in the external domains of several homologs of DDX3 (from yeast to human) and all described human DEAD-box proteins. DEAD-box helicases play pleiotropic functions within the cell by remodeling RNA:RNA and RNA:protein complexes or by functioning as RNA clamps for the assembly of large macromolecular complexes. Despite the high degree of conservation of the catalytic core and the mechanisms of RNA binding and ATP binding/hydrolysis in several members of the family, their functions are rather non-redundant probably due to the substrate specificity conferred by the N- and/or C-terminal domains surrounding the helicase core. Interestingly, several RNA helicases, including DDX3, have been identified as components of different RNP complexes and thus, associated with different biological processes involving RNA [2,15]. The presence of intrinsically disordered regions within the N- and C-termini may confer DEAD-box proteins the flexibility needed to interact with different partners in different RNP complexes in a spatiotemporal manner.

In the case of DDX3, the N-terminal domain allows interaction with the VACV K7 protein [35], eIF4E [36], IRF3 [38] and to be included in a complex together with CRM1 (Fig. 5), indicating an important role of this domain in establishing multiple interactions. Moreover, the N-terminal domain regulates the RNA-stimulated ATPase activity [11], stress granule assembly [37] and HIV-1 unspliced mRNA translation (Fig. 1) also indicating an important role of the N-terminal domain in regulating biological processes driven by this enzyme. Given the fact that neither the NES nor the eIF4E-binding domain seems to be involved in DDX3 function during HIV-1 gene expression (Fig. 6) [5,6], it is tempting to speculate that the intrinsically disordered N-terminal domain of DDX3 may first confer the ability to be incorporated into the CRM1-exported viral mRNP at the nuclear envelope and then the flexibility to promote the transition from an export mRNP to a translation one.

In this work we provide evidence for the interconnection between CRM1-dependent nuclear export and translation of the HIV-1 unspliced mRNA, two processes previously shown to require the catalytic activity of DDX3 [3,6]. This occurs through the intrinsically disordered N-terminal domain of DDX3, which allows the RNA helicase to be incorporated into the viral mRNP in a CRM1-dependent manner. Targeting the function of the N-terminal of DDX3 rather than its catalytic activity must be considered as a potential target for novel therapies against HIV.

Further work is needed to unveil the mechanisms involved in these processes.

Supplementary data to this article can be found online at http://dx.doi.org/10.1016/j.bbagrm.2016.03.009.

Conflict of interest

The authors declare that they do not have any conflict of interest.

Transparency document

The Transparency document associated with this article can be found in the online version.

Acknowledgments

The following material was obtained through the NIH AIDS Reagent Program, Division of AIDS, NIAD, NIH: H9 cells from Dr. Robert Gallo and Jurkat Clone E-61 from Dr. Arthur Weiss. This work was supported by CONICYT Chile through the FONDECYT Initiation Into Research Program N° 11121339 to RSR and N° 11140502 to FVE. This work was also supported by a grant from ANRS to TO. YPP and AGA are recipients of a Doctoral fellowship from the Graduate Program in Biomedical Sciences, Faculty of Medicine, Universidad de Chile. FGG is a recipient of a National Doctoral fellowship from CONICYT and PSR was a recipient of a Becas Chile Doctoral fellowship.

References

[1] F. Valiente-Echeverria, M.A. Hermoso, R. Soto-Rifo, RNA helicase DDX3: at the crossroad of viral replication and antiviral immunity, Rev. Med. Virol. (2015).
[2] R. Soto-Rifo, T. Ohlmann, The role of the DEAD-box RNA helicase DDX3 in mRNA metabolism, Wiley Interdiscip. Rev. RNA 4 (2013) 369–385 (Jul-Ago).
[3] V.S. Yedavalli, C. Neuveut, Y.H. Chi, L. Kleiman, K.T. Jeang, Requirement of DDX3 DEAD box RNA helicase for HIV-1 Rev-RRE export function, Cell 119 (2004) 381–392.
[4] J. Liu, J. Henao-Mejia, H. Liu, Y. Zhao, J.J. He, Translational regulation of HIV-1 replication by HIV-1 Rev cellular cofactors Sam68, eIF5A, hRIP, and DDX3, J. NeuroImmune Pharmacol. 6 (2011) 308–321.
[5] R. Soto-Rifo, P.S. Rubilar, T. Ohlmann, The DEAD-box helicase DDX3 substitutes for the cap-binding protein eIF4E to promote compartmentalized translation initiation of the HIV-1 genomic RNA, Nucleic Acids Res. 41 (2013) 6286–6299.
[6] R. Soto-Rifo, P.S. Rubilar, T. Limousin, S. de Breyne, D. Decimo, T. Ohlmann, DEAD-box protein DDX3 associates with eIF4F to promote translation of selected mRNAs, EMBO J. 31 (2012) 3745–3756.
[7] M.C. Lai, S.W. Wang, L. Cheng, W.Y. Tarn, S.J. Tsai, H.S. Sun, Human DDX3 interacts with the HIV-1 Tat protein to facilitate viral mRNA translation, PLoS One 8 (2013), e68665.
[8] M. Radi, F. Falchi, A. Garbelli, A. Samuele, V. Bernardo, S. Paolucci, F. Baldanti, S. Schenone, F. Manetti, G. Maga, M. Botta, Discovery of the first small molecule inhibitor of human DDX3 specifically designed to target the RNA binding site: towards the next generation HIV-1 inhibitors, Bioorg. Med. Chem. Lett. 22 (2012) 2094–2098.
[9] G. Maga, F. Falchi, M. Radi, L. Botta, G. Casaluce, M. Bernardini, H. Irannejad, F. Manetti, A. Garbelli, A. Samuele, S. Zanoli, J.A. Este, E. Gonzalez, E. Zucca, S. Paolucci, F. Baldanti, J. De Rijck, Z. Debyser, M. Botta, Toward the discovery of novel anti-HIV drugs. Second-generation inhibitors of the cellular ATPase DDX3 with improved anti-HIV activity: synthesis, structure–activity relationship analysis, cytotoxicity studies, and target validation, ChemMedChem 6 (2011) 1371–1389.
[10] A. Garbelli, M. Radi, F. Falchi, S. Beermann, S. Zanoli, F. Manetti, U. Dietrich, M. Botta, G. Maga, Targeting the human DEAD-box polypeptide 3 (DDX3) RNA helicase as a novel strategy to inhibit viral replication, Curr. Med. Chem. 18 (2011) 3015–3027.
[11] L.B. Epling, C.R. Grace, B.R. Lowe, J.F. Partridge, E.J. Enemark, Cancer-associated mutants of RNA helicase DDX3X are defective in RNA-stimulated ATP hydrolysis, J. Mol. Biol. (2015).
[12] M.C. Lai, W.C. Chang, S.Y. Shieh, W.Y. Tarn, DDX3 regulates cell growth through translational control of cyclin E1, Mol. Cell. Biol. 30 (2010) 5444–5453.
[13] P. Linder, F.V. Fuller-Pace, Looking back on the birth of DEAD-box RNA helicases, Biochim. Biophys. Acta 1829 (2013) 750–755.
[14] O. Cordin, J. Banroques, N.K. Tanner, P. Linder, The DEAD-box protein family of RNA helicases, Gene 367 (2006) 17–37.
[15] P. Linder, E. Jankowsky, From unwinding to clamping — the DEAD box RNA helicase family, Nat. Rev. Mol. Cell Biol. 12 (2011) 505–516.
[16] A. Jankowsky, U.P. Guenther, E. Jankowsky, The RNA helicase database, Nucleic Acids Res. 39 (2011) D338–D341.
[17] S. Rocak, P. Linder, DEAD-box proteins: the driving forces behind RNA metabolism, Nat. Rev. Mol. Cell Biol. 5 (2004) 232–241.
[18] A. Adachi, H.E. Gendelman, S. Koenig, T. Folks, R. Willey, A. Rabson, M.A. Martin, Production of acquired immunodeficiency syndrome-associated retrovirus in human and nonhuman cells transfected with an infectious molecular clone, J. Virol. 59 (1986) 284–291.
[19] R. Soto-Rifo, T. Limousin, P.S. Rubilar, E.P. Ricci, D. Decimo, O. Moncorge, M.A. Trabaud, P. Andre, A. Cimarelli, T. Ohlmann, Different effects of the TAR structure on HIV-1 and HIV-2 genomic RNA translation, Nucleic Acids Res. 1 (2012) 2653–2667 (Mar).
[20] A. Weiss, R.L. Wiskocil, J.D. Stobo, The role of T3 surface molecules in the activation of human T cells: a two-stimulus requirement for IL 2 production reflects events occurring at a pre-translational level, J. Immunol. 133 (1984) 123–128.
[21] D.L. Mann, S.J. O'Brien, D.A. Gilbert, Y. Reid, M. Popovic, E. Read-Connole, R.C. Gallo, A.F. Gazdar, Origin of the HIV-susceptible human CD4+ cell line H9, AIDS Res. Hum. Retrovir. 5 (1989) 253–255.
[22] S.E. Reed, E.M. Staley, J.P. Mayginnes, D.J. Pintel, G.E. Tullis, Transfection of mammalian cells using linear polyethylenimine is a simple and effective means of producing recombinant adeno-associated virus vectors, J. Virol. Methods 138 (2006) 85–98.
[23] L. Wang, S.J. Brown, BindN: a web-based tool for efficient prediction of DNA and RNA binding sites in amino acid sequences, Nucleic Acids Res. 34 (2006) W243–W248.
[24] M. Terribilini, J.D. Sander, J.H. Lee, P. Zaback, R.L. Jernigan, V. Honavar, D. Dobbs, RNABindR: a server for analyzing and predicting RNA-binding sites in proteins, Nucleic Acids Res. 35 (2007) W578–W584.
[25] Z. Dosztanyi, V. Csizmok, P. Tompa, I. Simon, IUPred: web server for the prediction of intrinsically unstructured regions of proteins based on estimated energy content, Bioinformatics 21 (2005) 3433–3434.
[26] P. Lieutaud, B. Canard, S. Longhi, MeDor: a metaserver for predicting protein disorder, BMC Genomics 9 (Suppl. 2) (2008) S25.
[27] R. Linding, R.B. Russell, V. Neduva, T.J. Gibson, GlobPlot: exploring protein sequences for globularity and disorder, Nucleic Acids Res. 31 (2003) 3701–3708.
[28] R. Linding, L.J. Jensen, F. Diella, P. Bork, T.J. Gibson, R.B. Russell, Protein disorder prediction: implications for structural proteomics, Structure 11 (2003) 1453–1459.
[29] J. Prilusky, C.E. Felder, T. Zeev-Ben-Mordehai, E.H. Rydberg, O. Man, J.S. Beckmann, I. Silman, J.L. Sussman, FoldIndex: a simple tool to predict whether a given protein sequence is intrinsically unfolded, Bioinformatics 21 (2005) 3435–3438.
[30] D.F. Purcell, M.A. Martin, Alternative splicing of human immunodeficiency virus type 1 mRNA modulates viral protein expression, replication, and infectivity, J. Virol. 67 (1993) 6365–6378.
[31] B. Wolff, J.J. Sanglier, Y. Wang, Leptomycin B is an inhibitor of nuclear export: inhibition of nucleo-cytoplasmic translocation of the human immunodeficiency virus type 1 (HIV-1) Rev protein and Rev-dependent mRNA, Chem. Biol. 4 (1997) 139–147.
[32] A.S. Zolotukhin, A. Valentin, G.N. Pavlakis, B.K. Felber, Continuous propagation of RRE(−) and Rev(−)RRE(−) human immunodeficiency virus type 1 molecular clones containing a cis-acting element of simian retrovirus type 1 in human peripheral blood lymphocytes, J. Virol. 68 (1994) 7944–7952.
[33] P. Gruter, C. Tabernero, C. von Kobbe, C. Schmitt, C. Saavedra, A. Bachi, M. Wilm, B.K. Felber, E. Izaurralde, TAP, the human homolog of Mex67p, mediates CTE-dependent RNA export from the nucleus, Mol. Cell 1 (1998) 649–659.
[34] O. Soderberg, M. Gullberg, M. Jarvius, K. Ridderstrale, K.J. Leuchowius, J. Jarvius, K. Wester, P. Hydbring, F. Bahram, L.G. Larsson, U. Landegren, Direct observation of individual endogenous protein complexes in situ by proximity ligation, Nat. Methods 3 (2006) 995–1000.
[35] S. Oda, M. Schroder, A.R. Khan, Structural basis for targeting of human RNA helicase DDX3 by poxvirus protein K7, Structure 17 (2009) 1528–1537.
[36] J.W. Shih, T.Y. Tsai, C.H. Chao, Y.H. Wu Lee, Candidate tumor suppressor DDX3 RNA helicase specifically represses cap-dependent translation by acting as an eIF4E inhibitory protein, Oncogene 27 (2008) 700–714.
[37] J.W. Shih, W.T. Wang, T.Y. Tsai, C.Y. Kuo, H.K. Li, Y.H. Wu Lee, Critical roles of RNA helicase DDX3 and its interactions with eIF4E/PABP1 in stress granule assembly and stress response, Biochem. J. 1 (2011) 119–129 (Jan).
[38] L. Gu, A. Fullam, R. Brennan, M. Schroder, Human DEAD box helicase 3 couples IkappaB kinase epsilon to interferon regulatory factor 3 activation, Mol. Cell. Biol. 33 (2013) 2004–2015.
[39] V.N. Uversky, The multifaceted roles of intrinsic disorder in protein complexes, FEBS Lett. (2015).
[40] M. Hogbom, R. Collins, S. van den Berg, R.M. Jenvert, T. Karlberg, T. Kotenyova, A. Flores, G.B. Karlsson Hedestam, L.H. Schiavone, Crystal structure of conserved domains 1 and 2 of the human DEAD-box helicase DDX3X in complex with the mononucleotide AMP, J. Mol. Biol. 372 (2007) 150–159.
[41] F.D. Bushman, N. Malani, J. Fernandes, I. D'Orso, G. Cagney, T.L. Diamond, H. Zhou, D.J. Hazuda, A.S. Espeseth, R. Konig, S. Bandyopadhyay, T. Ideker, S.P. Goff, N.J. Krogan, A.D. Frankel, J.A. Young, S.K. Chanda, Host cell factors in HIV replication: meta-analysis of genome-wide studies, PLoS Pathog. 5 (2009), e1000437.
[42] S.H. Mahboobi, A.A. Javanpour, M.R. Mofrad, The interaction of RNA helicase DDX3 with HIV-1 Rev-CRM1-RanGTP complex during the HIV replication cycle, PLoS One 10 (2015), e0112969.
[43] G. Hauk, G.D. Bowman, Formation of a trimeric Xpo1-Ran[GTP]-Ded1 exportin complex modulates ATPase and helicase activities of Ded1, PLoS One 10 (2015), e0131690.
[44] B. Tieg, H. Krebber, Dbp5 — from nuclear export to translation, Biochim. Biophys. Acta 1829 (2013) 791–798.
[45] J. Banroques, O. Cordin, M. Doere, P. Linder, N.K. Tanner, Analyses of the functional regions of DEAD-box RNA "helicases" with deletion and chimera constructs tested in vivo and in vitro, J. Mol. Biol. 413 (2011) 451–472.